

A three-dimensional receiver function migration method imaging the crustal structure in Sichuan-Yunnan region, Southwest China

Shizhuo Mao¹ (miao@mail.ustc.edu.cn), Shihua Cheng¹, Xiao Xiao¹, Jianping Wu² and Lianxing Wen³

¹ Laboratory of Seismology and Physics of Earth's Interior, School of Earth and Space Sciences, University of Science and Technology of China

² Institute of Geophysics, China Earthquake Administration, Beijing, China

³ Department of Geosciences, Stony Brook University



Stony Brook
University

ADVANCING
EARTH AND
SPACE SCIENCE
AGU100
S21D-0534

Introduction

The Sichuan-Yunnan region lies within a complex tectonic framework and is one of the most seismically active regions in the continental China. A high-resolution image of the crustal structure of the region is of importance in understanding the crustal deformation since the Indo-China collision, the evolution of Cenozoic slip faults, and possible crustal decoupling in the eastern Tibet. We develop a three-dimensional (3D) receiver function migration method and apply the method to imaging the 3D crustal structure in the Sichuan-Yunnan region.

Theory & Method

Seismic Migration is often used to image velocity interfaces. We apply a poststack phase screen method, which is a high efficient one-way wave equation method in forward modeling. In this method, receiver functions are propagated downward, taking the 1st order Padé approximation of 3D scalar wave equation, calculated in the frequency-domain.

Starting from the scalar wave equation

$$\left[\frac{\partial^2}{\partial x^2} + \frac{\partial^2}{\partial y^2} + \frac{\partial^2}{\partial z^2} + \frac{\omega^2}{c^2(x, y, z)} \right] u(x, y, z) = 0 \quad (1)$$

where $u(x, y, z)$ is the wave field. The above equation can be divided into two one-way wave equations, one for forward propagation and the other for backward propagation. By defining a reference velocity $c_0 = c(x, y, z)n(x, y, z)$ and a reference wave-number $k_0 = \omega/c_0$, the forward propagated's governing equation is

$$\frac{\partial u(x, y, z)}{\partial z} = i \sqrt{n^2 k_0^2 + \frac{\partial^2}{\partial x^2} + \frac{\partial^2}{\partial y^2}} u(x, y, z) \quad (2)$$

Padé approximation is applied to calculate the expansion for 1st order expansion, we have

$$\frac{\partial u(x, y, z)}{\partial z} = ik_0 \left[\frac{1}{2} n^2 k_0^2 \left(\frac{\partial^2}{\partial x^2} + \frac{\partial^2}{\partial y^2} \right) \right] u(x, y, z) \\ + \frac{1}{1 + \frac{1}{4} \left(\frac{1}{n^2 k_0^2} \left(\frac{\partial^2}{\partial x^2} + \frac{\partial^2}{\partial y^2} \right) \right)} u(x, y, z) \quad (3)$$

If the wave field is expressed as a stack of plane wave, we have

$$\frac{\partial u(z, k_{0x}, k_{0y})}{\partial z} = i \left[k_{0z} - k_0 \left(\frac{\delta c}{c} \right) - k_0 \frac{\frac{1}{2} \left(\frac{1}{n^2} \right) - 1}{k_0^2} \frac{k_{0x}^2 + k_{0y}^2}{k_0^2} \right] U(z, k_{0x}, k_{0y}) \quad (4)$$

where $\delta c = c - c_0$, k_{0x} , k_{0y} are the transverse wavenumber and k_{0z} is the vertical wavenumber. $U(z, k_{0x}, k_{0y})$ is the amplitude of the plane wave. Under the thin-slab assumption, a forward-propagated frequency-wavenumber domain equation is obtained.

$$U(k_x, k_y, z_{i+1}, \omega) = e^{ik_z(z_{i+1}-z_i)} \cdot FT_x FT_y \left[\exp \left(-i \left(\frac{\partial c(x, y, z_i)}{c(x, y, z_i)} + \frac{1}{2} \frac{k_x^2 + k_y^2}{k_0^2} \frac{\partial c(x, y, z_i)}{c_0(z_i)} \right) k_0(z_{i+1} - z_i) \right) u(x, y, z_i, \omega) \right] \quad (5)$$

Our method employs the principle that the reverse-time migrated converted phases from an interface shall interfere at the interface at zero time. A range of different depths of velocity interfaces is assumed. Receiver function profiles are stacked after CCP move-out correction and are migrated to different corresponding depths. The final migration image is obtained by combining all assumed-depth images.

Synthetic Tests

We apply the 3D finite difference algorithm to perform a number of synthetic experiments in order to test the validity and effectiveness of the phase screen method.

With each velocity model, we calculate 50 receiver functions with different azimuths or angles of (plane wave) incidence before CCP stackings and migration.

Two models, one defined by a 2D Gaussian function and the other defined by a step function, are tested to investigate the undulation and discontinuities of velocity interfaces respectively. Migration results show that both two models can be well imaged. Images for different receiver distances, obtained after receiver function waveform interpolated, suggest that poor distribution affects the migration results by creating 'fake' discontinuities of velocity interfaces. To investigate the influence of the existence of sediments near the surface, migration with 4.8 km sediment model is performed, indicating that thick sediment may lead to noisy multiples.

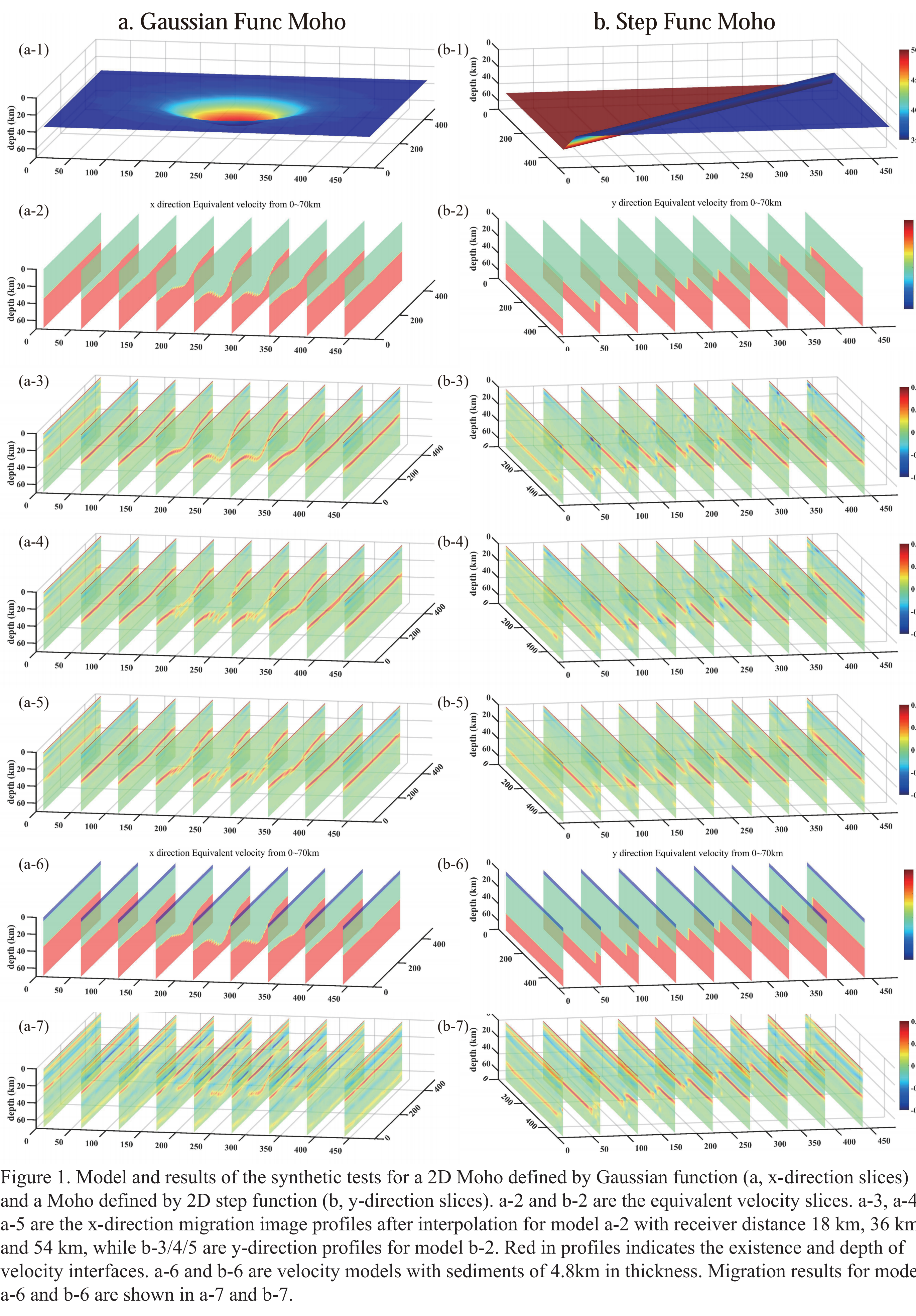


Figure 1. Model and results of the synthetic tests for a 2D Moho defined by Gaussian function (a, x-direction slices) and a Moho defined by 2D step function (b, y-direction slices). a-1 and b-1 are the equivalent velocity slices. a-3, a-4, a-5 are the x-direction migration image profiles after interpolation for model a-2 with receiver distance 18 km, 36 km and 54 km, while b-3/4/5 are y-direction profiles for model b-2. Red in profiles indicates the existence and depth of velocity interfaces. a-6 and b-6 are velocity models with sediments of 4.8km in thickness. Migration results for model a-6 and b-6 are shown in a-7 and b-7.

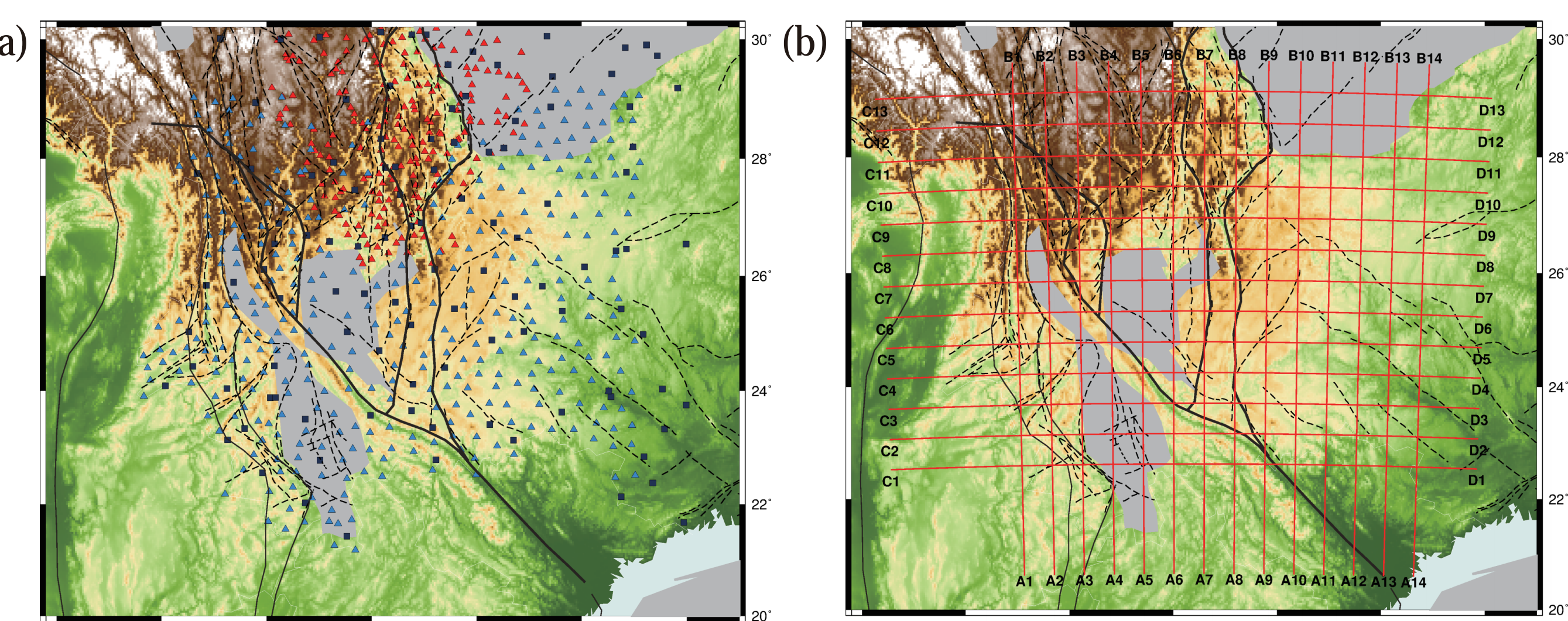


Figure 2. Map of stations in longitude and latitude (a) and selected profiles (b). In 2a, X1 Array receivers are labelled in light blue triangles, T1 stations are in red triangles and the CNSN stations are labelled in dark blue squares. Black solid lines and dashed lines show the faults in Sichuan-Yunnan region. Three major basins (Sichuan Basin, Chuxiong Basin and Simao Basin from Northeast to Southwest) in this region are marked in gray. In 3b, red lines give the selected 27 profiles for illustration in Fig. 3.

Acknowledgment

CNSN waveform data for this study are provided by Data Management Centre of China National Seismic Network at Institute of Geophysics, China Earthquake Networks Center. ChinArray waveform data (T1 and X1) are provided by China Seismic Array Data Management Center at Institute of Geophysics, China Earthquake Administration.

Data Application Results

In the application of imaging the 3D crustal structure in the Sichuan-Yunnan region, we employ 193541 P-wave receiver functions obtained from 565 seismic stations in the Sichuan-Yunnan region, including 56 permanent stations from China National Seismic Network (CNSN) and 509 temporary stations from ChinArray, for seismic events occurring in an epicentral distance range from 30° to 95° and with a magnitude (Mw) above 5.5 (Fig 2). The obtained crustal structure images (Fig 3) exhibit an overall crustal thickening from south to north and from east to west, with significant Moho depth variations across the boundary of the Tibetan Plateau. Prominent 'mid-crustal seismic discontinuities', with a depth ranging from 15 km to 20 km, is also present at the southern edge of the Sichuan Basin and at the north-eastern edge of the Chuxiong Basin. These 'interfaces' may also be caused by the thick sediment, leading to a blurred imaging of Moho as well.

Conclusions

We develop a 3D screen method receiver function migration method to image Moho and other crustal structures. Tests of synthetics indicate that our new method works well in imaging 3D Moho and other shallow structures, even in the regions with large depth offsets of the interfaces. A clear 3D crustal receiver function migration image is obtained in Sichuan-Yunnan Region employing ChinArray & CNSN data.

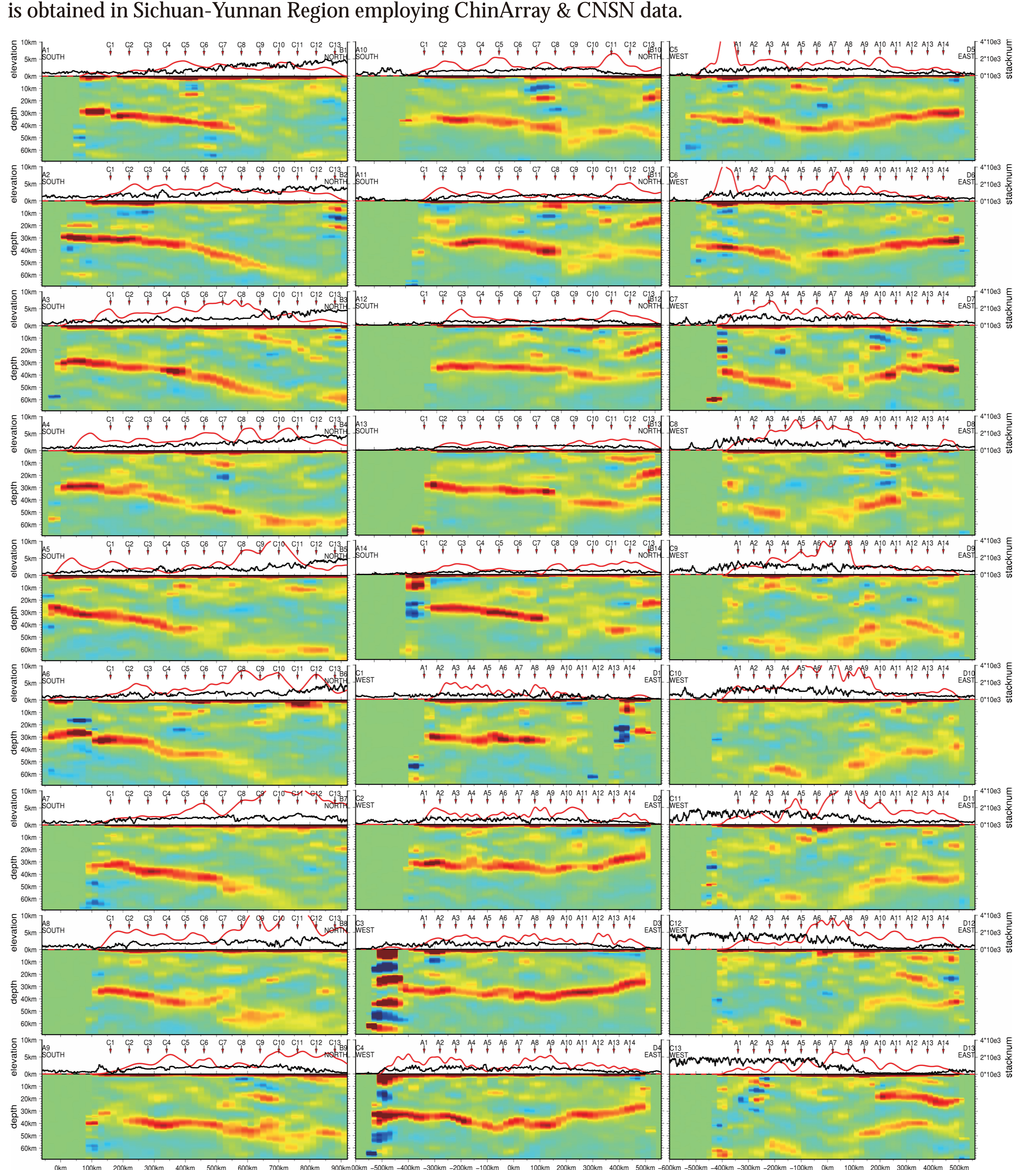


Figure 3. Profiles of 3D migration results. Red gives higher migration image value, indicating a higher possibility of the existence of interfaces. Red curves are the smoothed bin-stack numbers of CCP traces. Black lines shows the elevations along the profiles. Vp/Vs velocity models in the migration are obtained by body-wave polarization, Rayleigh-wave ellipticity and receiver functions (S23C-0530, AGU 2018).